Agricultural and Forest Meteorology 339 (2023) 109575

Contents lists available at ScienceDirect

Agricultural and Forest Meteorology

journal homepage: www.elsevier.com/locate/agrformet

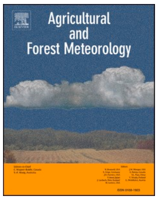

The impact of warming climate on Himalayan silver fir growth along an elevation gradient in the Mt. Everest region

Narayan Prasad Gaire [a,b,#], Zaw Zaw [a,c,#], Achim Bräuning [d], Jussi Grießinger [d], Bimal Sharma [a], Prabina Rana [e], Sanjaya Bhandari [f], Saroj Basnet [g], Ze-Xin Fan [a,c,*]

[a] CAS Key Laboratory of Tropical Forest Ecology, Xishuangbanna Tropical Botanical Garden, Chinese Academy of Sciences, Menglun, Mengla, Yunnan 666303, China
[b] Department of Environmental Science, Patan Multiple Campus, Tribhuvan University, Lalitpur 44700, Nepal
[c] Ailaoshan Station of Subtropical Forest Ecosystem Studies, Xishuangbanna Tropical Botanical Garden, Chinese Academy of Sciences, Jingdong, Yunnan 676209, China
[d] Institute of Geography, University of Erlangen-Nürnberg, Erlangen 91058, Germany
[e] Nepal Academy of Science and Technology, Khumaltar, Lalitpur 3323, Nepal
[f] Department of Earth and Environmental System, Indiana State University, Terre Haute, IN 47809, USA
[g] Institute of Botany and Landscape Ecology, University of Greifswald, Greifswald 17489, Germany

ARTICLE INFO

Keywords:
Climate change
Climate sensitivity
Elevation gradient
Growth trend
Himalayan silver fir (*Abies spectabilis*)
Tree ring

ABSTRACT

The impacts of rapid climate change in the Himalayan region on growth and sensitivity of tree species across their entire elevation distribution range are not well understood. This study investigates the growth and climate sensitivity of the endemic species Himalayan silver fir (*Abies spectabilis*, D.Don) along an elevation gradient in the sub-alpine belt in the Mt. Everest region. We developed tree ring-width chronologies, spanning 98 to 310 years, from six sites along an elevation gradient (3400–4100 m a.s.l.). The growth of Himalayan silver fir is primarily limited by low temperatures during the growing season and moisture availability during spring. Significant positive correlations were found between tree growth and mean, minimum and maximum temperatures for most parts of the vegetation period except spring. In contrast, significant positive correlations are apparent for precipitation, self-calibrated Palmer drought severity index (scPDSI), and standardized precipitation-evapotranspiration index (SPEI) during the spring season (March–May) at most of the elevations except for the upper treeline site. Thus, low summer temperatures are the primary limiting factor at all investigated elevations, while moisture supply during spring triggers growth variations at low- to mid-elevations. The long-term growth trends of *A. spectabilis* have decreased at low- to mid-elevation sites but increased at the treeline during the period 1981–2011. Warming and intensified moisture stress during spring could have negative effects on tree growth, potentially resulting in growth decline and forest dieback at middle and low elevations. These findings emphasize the importance of understanding the vulnerability of forests at middle and low elevations to future climate change.

1. Introduction

Global climate change is a crucial concern for biodiversity hotspots such as the Himalaya (IPCC, 2022). The region is experiencing rapid climate warming and increased frequency and magnitude of extreme precipitation and drought events, as documented in various studies (Qi et al., 2013; IPCC, 2014; Agarwal et al., 2016; Sun et al., 2017; Talchabhadel et al., 2018; Gaire et al., 2019, 2022). The impacts of climate change in the Himalaya are reflected in changes in phenology, distribution ranges of tree species, treeline dynamics, sub-nival greening, and shrub encroachment at high altitudes (Shrestha et al., 2012; Brandt et al., 2013; Telwala et al., 2013; Dolezal et al., 2016; Gaire et al., 2017; Sigdel et al., 2018; Anderson et al., 2020). Warming climate leads to geographic shifts in tree growth limitations, with a significant decrease in temperature sensitivity at cold-dry sites and an increase in moisture sensitivity worldwide (Babst et al., 2019). This puts the forests and biodiversity of the Himalayan region at further risk, as the ecosystems are vulnerable and prone to climate-induced vegetation shifts (Gonzalez et al., 2010; Anderson et al., 2020). However, predicting the impacts of climate warming on plant communities can be more complex than

---

* Corresponding author.
E-mail address: fanzexin@xtbg.org.cn (Z.-X. Fan).
[#] These authors contributed equally to this work.

https://doi.org/10.1016/j.agrformet.2023.109575
Received 4 December 2022; Received in revised form 15 April 2023; Accepted 19 June 2023

expected due to interactions among complex environmental conditions (Ferrarini et al., 2014). Although studies on the effects of climate change on forest tree species along their entire elevation range are sparse in the Himalayan region, they are essential for understanding biological responses to climate change (Anderson et al., 2020).

Studying species' responses to climate change along elevation gradients is valuable since many biophysical parameters vary with altitude, allowing for the investigation of sensitivity, response, and coping organisms (Körner, 2012). The Mt. Everest region, with one of the world's longest elevation gradients, is a crucial component of the Himalayan biodiversity hotspot and serves as an ideal location for assessing climate change impacts on tree growth along species' altitudinal distribution ranges. In the central Himalaya, the annual mean temperature decreases by about 0.5 °C per 100 m increase in elevation (DHM, 2017). Recent studies suggest that warming is elevation-dependent in the Himalaya, with higher elevations experiencing greater temperature increases than lower elevations (Liu et al., 2009; Thakuri et al., 2019; Karki et al., 2020). This may lead to more favorable growth conditions for tree species adapted to the colder environment and result in their expansion (IPCC, 2014). Understanding tree growth responses to ongoing climate change throughout their entire elevation gradient is essential for biodiversity conservation and natural resource management.

Previous studies from different mountain systems worldwide suggest that the response of tree growth to climate change along their elevation distribution range can vary depending on species, local site conditions, and climate (Lyu et al., 2016; Babushkina et al., 2018; Liu et al., 2018; Gaire et al., 2020). Generally, trees growing at their lower distribution limit in semi-arid areas are more sensitive to precipitation fluctuations (Fan et al., 2009; Lv and Zhang, 2012; Kharal et al., 2017; Panthi et al., 2020), while those at their upper limit are more sensitive to temperature changes (Fan et al., 2009; Lv and Zhang, 2012; Kharal et al., 2017; Shrestha et al., 2017; Wang et al., 2017; Gaire et al., 2020; Panthi et al., 2020). However, some species in high mountain areas show similar responses to temperature across their elevation distribution range (Liang et al., 2010; Gao et al., 2013; Gaire et al., 2020). Dendrochronological studies from different regions of High Asia suggest that species growing in temperature-limited areas are responding to global warming through enhanced growth, while tree growth in moisture-limited areas can increase, remain stable, or decrease, depending upon moisture availability and prevailing drought situations (IPCC, 2014; Kharal et al., 2017; Shrestha et al., 2017; Liang et al., 2019; Rai et al., 2019; Gaire et al., 2020).

Initiatives have already been undertaken to assess the response of Himalayan silver fir along its elevation distribution range in the Himalaya, but conclusive evidence is lacking due to diverse growth trends and climate-growth response (Kharal et al., 2014, 2017; Shrestha et al., 2015; Rai et al., 2019; Gaire et al., 2020; Panthi et al., 2020). Some sites have reported increased or decreased tree growth in response to observed warming trends throughout the elevation range (Gaire et al., 2020; Panthi et al., 2020). In other sites, enhanced tree growth in the upper areas and decreasing growth in the lower areas (Rai et al., 2019; Panthi et al., 2020), or no clear growth trend along the elevation were found (Kharal et al., 2014, 2017; Shrestha et al., 2015). As Himalayan silver fir is a species of high ecological importance, there is an urgent need for a denser network of studies from new areas to clarify its elevation-dependent response to climate change.

Climate change is significantly impacting tree growth and vegetation dynamics in the Mt. Everest region of the Himalaya (Byers, 2007; Fukui et al., 2007; Benn et al., 2012; Thakuri et al., 2014; DNPWC, 2015; Sigdel et al., 2018). Several promising tree taxa with known dendroclimatic potential, including *Abies spectabilis, Betula utilis, Juniperus* species, *Tsuga dumosa*, and *Rhododendron* species, inhabit the Mt. Everest region (Shrestha and Jha, 2010; Liang et al., 2014; DNPWC, 2015; Gaire et al., 2017). Among these, *A. spectabilis* (Himalayan Silver fir) was recognized as an indicator species due to its wide geographical and elevational distribution range in the Himalaya. Himalayan silver fir is the dominant species of the upper temperate to subalpine forest belt and also shows treeline dynamics in response to climate change (Chhetri and Cairn, 2016; Gaire et al., 2017; Sigdel et al., 2018; Panthi et al., 2020).

A dendroecological study on fir growth from the northern declivity (Tibetan Plateau side) of Mt. Everest found a temperature signal at higher elevation and a moisture signal at lower elevation belt (Lv and Zhang, 2012). However, no study has yet investigated the response of a tree species along with its entire elevation distribution range in the southern declivity of the world's highest elevation gradient, the Mt. Everest region. Thus, this study aims to investigate the growth and climate sensitivity of *Abies spectabilis* (Himalayan silver fir) along an elevation gradient in the Sagarmatha (Mt. Everest) National Park (SNP). This study intends to identify the key climatic factors limiting the growth of *A. spectabilis* along its elevational distribution range and assess the changes in long-term tree growth rates at various elevations. As the study site is located in the subalpine to alpine elevation belt (above 3, 000 m a.s.l.), we hypothesize that trees are sensitive and highly responsive to changes in temperature. Similarly, Himalayan silver fir trees are also sensitive to precipitation, as the Inner Himalayan valleys act as a natural barrier for precipitation (rain shadow effect) in the Himalaya. The study's findings may provide a better understanding of different growth trajectories and climate responses of Himalayan silver fir along an elevation gradient under the climate change scenario.

2. Materials and methods

2.1. Study area

The study area is situated in the Sagarmatha National Park (SNP), an area of 1,148 km^2 (Fig. 1). The SNP is a high mountain natural reserve characterized by a vast elevational range of 2,845 to 8,848.86 m a.s.l. (DNPWC, 2015). The SNP is a UNESCO World Natural Heritage Site due to its diverse natural, cultural and biological features (DNPWC, 2015). It contains various forest ecosystems, ranging from temperate to alpine and nival belts (Jha, 2010; DNPWC, 2015). The study area focused on mixed forests dominated by *A. spectabilis*, which is associated with *Rhododendron* species at lower and middle elevations (Shrestha and Jha, 2010). In the timberline region, it is associated with *B. utilis, Rhododendron campanulatum, R. campylocarpum*, and *Acer* species, while the treeline ecotone community includes *Abies, Betula, Rhododendron, Sorbus*, and *Juniperus* species (DNPWC, 2015; Gaire et al., 2015, 2017).

2.2. Regional climate conditions

The climate of the SNP is primarily influenced by the Indian summer monsoon, although arid conditions may occur in the inner valleys of the Himalaya due to the barrier effect of high mountains on the monsoon winds (DHM, 2017; Talchabhadel et al., 2019). The winter season is characterized by extremely cold temperatures, with minimum temperatures below −10 °C at Pyramid station (located at 5,050 m a.s.l.) (Fig. 2a). High-elevation area receives snowfall during both winter and spring seasons (Salerno et al., 2015). Local instrumental climate measurements reveal a continuous increase in temperature in the Mt. Everest region over the last few decades, while precipitation varies across different sites and stations (Salerno et al., 2015; Gaire et al., 2017). Gridded climate data (CRU 4.03, 1951–2017) also show a generally increasing temperature but no significant trend in precipitation, except for some months or seasons (Fig. 2b). Fig. 2b provides detailed information on the respective trends in different climate parameters.

2.3. Sample collection, preparation, and data acquisition

Tree-ring samples were collected in 2012 and 2016. The sampling covered the entire elevation distribution range of *A. spectabilis* up to the upper treeline (Fig. 1; Table 1), with at least 200-meter elevation

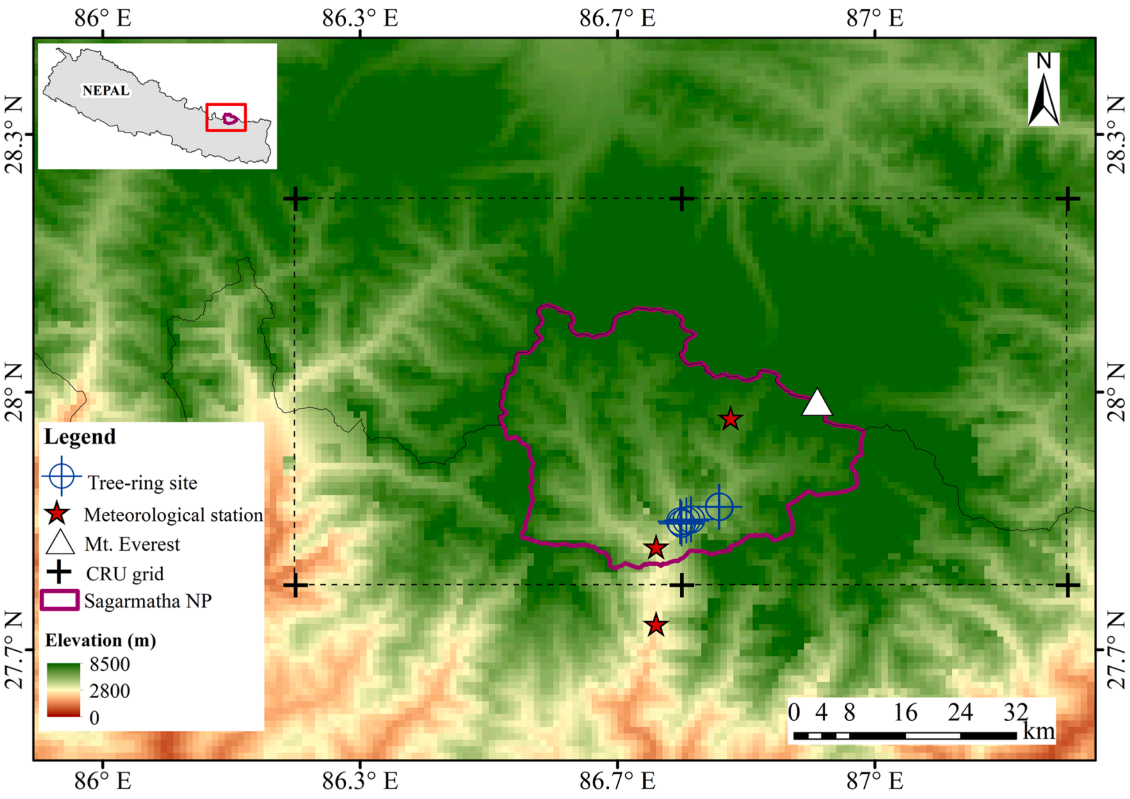

Fig. 1. Location map of the study area showing tree-ring sampling sites, meteorological stations, and CRU grid points.

differences between adjacent sampling sites. Following dendrochronological sampling procedures (Fritts, 1976; Speer, 2010), one to two cores were collected from healthy, dominant, or co-dominant trees. Cores were sampled parallel to the contour slope whenever possible. A total of 300 increment cores were collected from 165 trees across six sampling sites (Table 1).

The tree-ring cores were air-dried and mounted in wooden frames with the transverse surface facing up. Wood surfaces were manually or machine-polished using sanding papers of varying grit sizes (120–800 grits) until ring boundaries and anatomical features are clearly visible under the microscope. Ring widths were measured with a stereo-microscope at 0.01 mm resolution using a digital linear measurement system (LINTAB5^{TM}) attached to TSAP-win software (Rinn, 2010). To identify missing and false rings, cross-dating was performed using the TSAP-win software, with missing or false rings identified through visual and statistical checks (Gleichläufigkeit, t-values, and cross-date index) and errors corrected after rechecking the samples and data (Rinn, 2010). Series less than 40 years or with highly individualistic growth behavior were excluded from further analyses. COFECHA was used to verify the quality of cross-dating and make the necessary correction (Holmes, 1983). To identify growth during extreme climate events, a pointer year analysis was conducted using the '*pointRes*' package in R (van der Maaten-Theunissen et al., 2015).

2.4. *Standardization and chronology development*

Tree-ring series contain long-term trends related to biological effects as well as to climate (Fritts, 1976; Speer, 2010). To remove biological growth trends while retaining climate signal, tree-ring series were detrended using the signal-free approach (Melvin and Briffa, 2008), with the RCSigFree program (https://www.ldeo.columbia.edu/tree-ring-laboratory/resources/software). This method preserves low- to medium-frequency signals while removing the biological growth trend. An age-dependent spline curve with age-related variance stabilization was used for detrending. The quality of the resulting tree-ring chronology was assessed using mean inter-series correlation (Rbar) (Briffa, 1995) and expressed population signal (EPS) statistics (Wigley et al., 1984). Principal Component Analysis (PCA) was conducted to identify common signals captured in the chronologies and cluster analysis was performed using the group-average linkages method to assess the relationships among the chronologies. The '*FactoMineR*' (Lê et al., 2008) and '*ggdendro*' (de Vries and Ripley, 2022) packages in R were used to conduct PCA and cluster analyses, respectively.

2.5. *Climate-growth relationships*

For investigating the climatic response of tree growth, climate data from the nearest meteorological stations are desirable (Fritts, 1976; Speer, 2010). However, climate data from the nearest meteorological stations (Namche and Pyramid) are too short (less than 30 years) and incomplete for reliable statistical analysis. Therefore, we extracted the CRU half-degree resolution monthly gridded climate data (CRU TS 4.03; Harris et al., 2020) from the KNMI Climate Explorer (Trouet and Oldenborgh, 2013). Data from six grid points (27.5–28.5 °N and 86–87.5 °E) covering the full study area were averaged to represent regional climate variability. The CRU climate data includes monthly minimum, maximum and mean temperatures, precipitation, standardized precipitation evapotranspiration index (SPEI), and self-calibrated Palmer drought severity index (scPDSI). Bootstrapped (Pearson's) correlation coefficient was calculated between tree-ring standard chronologies and climate variables for the common period of 1951–2011 using the '*treeclim*' R package (Zang and Biondi, 2015). Correlations were calculated for a 13-month climatic window starting from October of the previous growth year until October of the current growth year. Seasonal influence of climate was also checked for three seasons: winter (DJF), spring (MAM), and summer (JJAS). To identify the influence of seasonal temperature and precipitation as the main growth-limiting factor, seasonal correlation analysis was conducted using the '*seascorr*' function in the '*treeclim*' R package (Zang and Biondi, 2015). This analysis was performed using partial correlations by taking temperature as the primary

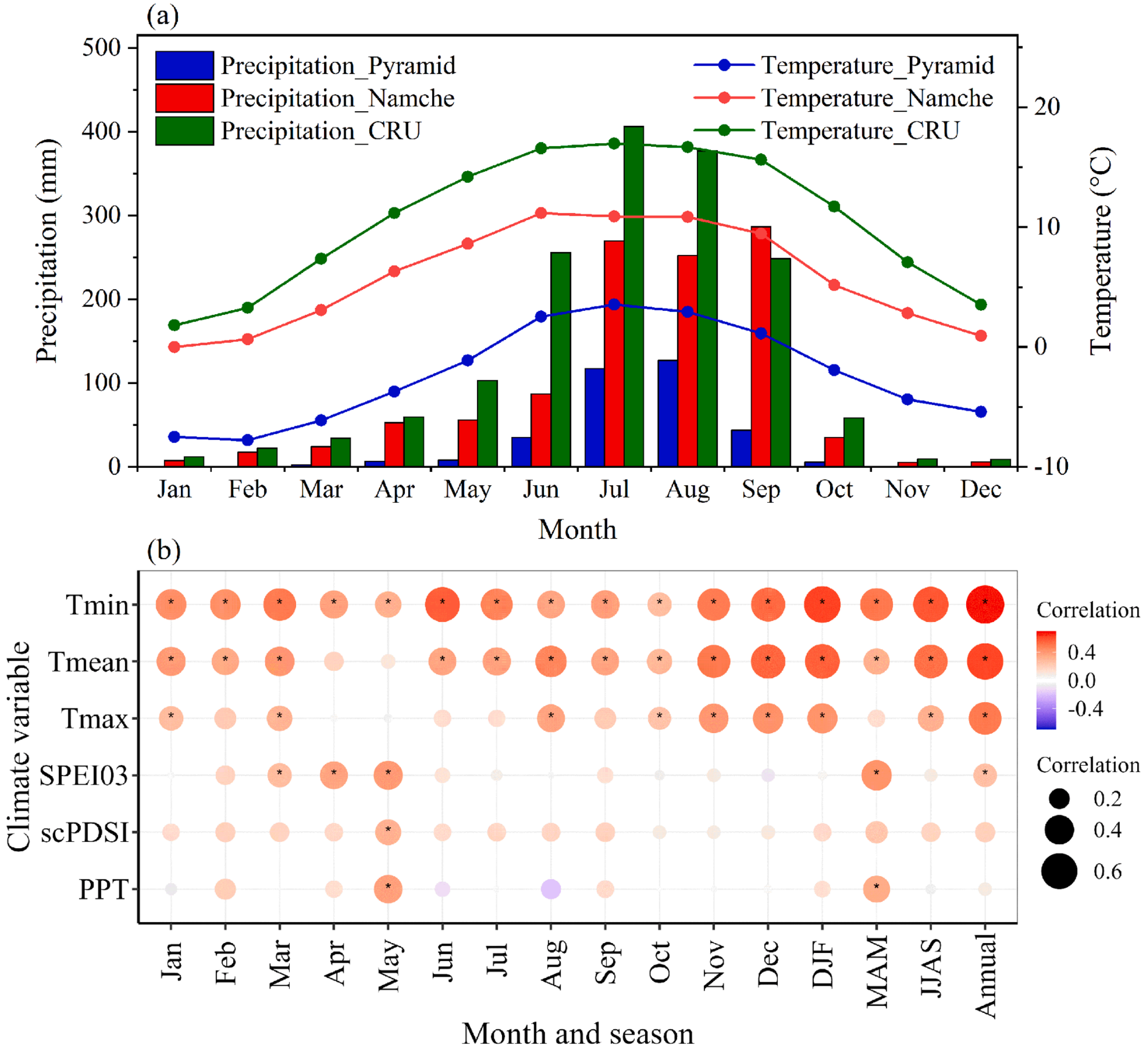

Fig. 2. (a) Monthly climate of the study area derived from nearest meteorological stations (Namche and Pyramid) and CRU gridded data. (b) Positive or negative trends (significant Pearson's correlation coefficient indicated by * symbol) in the CRU climate data covering the study region for the period 1951–2017. PPT, scPDSI, SPEI03, Tmax, Tmean, and Tmin indicate precipitation, self-calibrated Palmer drought severity index, three-month standardized precipitation-evapotranspiration index, maximum temperature, mean temperature, and minimum temperature, respectively. DJF, winter season; MAM, spring season; JJAS, summer season.

factor and precipitation as the secondary factor, and vice-versa. The temporal stability of the climatic response (Wilmking et al., 2020) was checked by performing a moving correlation analysis between the chronology and climate using a 30-year window with a one- and five-year window offset in the '*treeclim*' R package (Zang and Biondi, 2015).

2.6. Basal area increment and long-term growth trends

Basal area increment (BAI) is a useful measure of long-term trends in tree growth (Phipps and Whiton, 1988) as it reflects total biomass production, and can provide a stable representation of tree growth (Leblanc, 1990). Ring-width measurements were converted into tree BAI using the following formula with the function '*bai.out*' in the R package '*dplR*' (Bunn, 2008):

$$\mathrm{BAI}_t = \pi\left(R_t^2 - R_{t-1}^2\right) \tag{1}$$

where R_t and R_{t-1} are the tree radii at the year t and $t-1$ of tree-ring formation. Individual tree BAI series were averaged for each site to develop a site-level BAI chronology.

To remove age- and size-related trends, the derived BAIs were detrended using generalized additive mixed models (GAMMs) (Wood, 2017). BAI values were log-transformed to improve the normality of their distributions. The GAMMs had the following structure:

$$\log(\mathrm{BAI}) \sim \log(\mathrm{BA}) + s(\mathrm{Age}) + (1|\mathrm{TreeID}) + \mathrm{corAR1} \tag{2}$$

where BA is the basal area, Age is the cambial age of a tree, and TreeID is the random factor of trees. The "s" represents the cubic regression spline for smoothing variables. An autoregressive term, AR1 (autoregressive order p = 1, moving average order q = 0), was added to account for temporal autocorrelation. Separate GAMMs were constructed for each elevation belt (site) using the '*mgcv*' package (Wood, 2017). The BAI residuals were calculated as:

$$\mathrm{BAI}_{\mathrm{residuals}} \sim \log\left(\mathrm{BAI}_{\mathrm{observed}}\right) - \log\left(\mathrm{BAI}_{\mathrm{predicted}}\right) \tag{3}$$

The trends of BAI residuals for each site were assessed by linear

Table 1
Site and chronology statistics of *Abies spectabilis* from the Mt. Everest region. The dendrochronological statistics were computed based on the span of each chronology. MS, AC1, Rbar, and EPS were calculated after detrending. AGR, annual radial growth rate; SD, standard deviation; MS, mean sensitivity; AC1, autocorrelation of level 1; Rbar, mean inter-series correlation; EPS, expressed population signal.

Statistics	Site code					
	3400m	3500m	3600m	3800m	3850m	4100m
Latitude	27.83	27.83	27.83	27.84	27.85	27.85
Longitude	86.75	86.75	86.76	86.76	86.80	86.78
Elevation (m a.s.l.)	3400	3500	3600	3800	3850	4100
Trees	25	18	26	21	39	36
Cores	34	25	37	31	53	54
First year	1846	1876	1711	1929	1886	1838
Last year	2015	2015	2015	2015	2011	2011
Mean age (year)	84	107	129	76	69	89
Mean AGR (mm/yr)	2.29	1.75	1.62	2.28	2.02	1.44
Median AGR (mm/yr)	1.95	1.55	1.40	1.93	2.34	1.36
Min AGR (mm/yr)	1.27	0.93	0.54	1.13	1.37	0.53
Max AGR (mm/yr)	4.25	3.60	3.73	3.22	3.94	2.60
SD AGR (mm/yr)	1.24	0.86	0.91	1.37	0.68	0.51
MS	0.187	0.175	0.227	0.168	0.14	0.141
AC1	0.43	0.53	0.44	0.50	0.53	0.61
Rbar	0.311	0.436	0.497	0.410	0.471	0.335
EPS	0.989	0.957	0.979	0.981	0.938	0.977

mixed-effects models (LME) using the '*nlme*' package in R (Pinheiro et al., 2021) as:

$$\mathrm{BAI}_{\mathrm{residuals}} \sim \mathrm{Year} + (1|\mathrm{TreeID}) + \mathrm{corAR1} \tag{4}$$

where $\mathrm{BAI}_{\mathrm{residuals}}$ is the basal area increment residuals after GAMM detrending and TreeID is the individual tree as the random factor.

The effect of all sites (elevation belts) in interaction with the calendar year as covariates on $\mathrm{BAI}_{\mathrm{residuals}}$ was analyzed to detect differences in growth trajectories between elevations using the following linear mixed-effects models (LME):

$$\mathrm{BAI}_{\mathrm{residuals}} \sim \mathrm{Year} \times \mathrm{Site} + (1|\mathrm{TreeID}) + \mathrm{corAR1} \tag{5}$$

where Year and Site are fixed factors, and Year × Site is an interaction between two fixed factors. To detect changes in long-term growth trends, the '*segmented*' R package (Muggeo, 2017) was used to identify breakpoints in BAI residuals of individual series. Based on the density distribution of breakpoints, the year with the mean frequency of breakpoints for all trees was selected to split the BAI residuals into two sub-periods for growth trend analysis. Annual climate trends were also analyzed to assess the regional climatic condition which may influence the long-term trends in tree growth.

3. Results

3.1. Growth patterns of A. spectabilis along the elevation gradient

The dendroclimatic utility of *A. spectabilis* was high, with moderate mean sensitivity, high standard deviation, low autocorrelation, high EPS, and a moderate Rbar (Table 1). The average radial growth rates ranged from 1.44 mm/yr to 2.29 mm/yr, with the highest annual radial growth rate (4.25 mm/yr) found at 3400 m a.s.l., and the minimum (0.53 mm/yr) at the treeline site (4100 m a.s.l.). Overall, radial growth rates decreased from low to high elevations (Table 1). No persistent trends in the chronology statistics (Rbar and EPS) were apparent along the elevation gradient, except for AC1 which increased with increased elevation (Table 1). Tree-ring chronologies exhibited similar short- and long-term growth patterns, but medium-term (decadal) growth sometimes varies between sites (Fig. 3). Pointer year analysis revealed that some negative (1959, 1984, and 1999) and positive (1998) pointer years were shared among all elevations, while others were site-specific (Fig. S2).

The PCA analysis, which includes all chronologies for the common period (1951–2011), indicated that PC#1 and PC#2 explained 65.7% and 18.0% of the common variance, respectively (Fig. 4a). PC#1 represented common growth variations sharing by different site chronologies, whereas PC#2 mainly reflected differences among elevations (Fig. 4a). Using cluster analysis, we grouped all chronologies into two sub-groups: a treeline group (4100m and 3850m) and a low- to mid-elevation group (3400m, 3500m, 3600m, and 3800m) (Fig. 4b).

3.2. Climate-growth relationships

Pearson's correlations with climatic variables indicated that tree growth of *A. spectabilis* is primarily limited by low temperatures prior to and during the growing season, and secondarily by moisture availability during the spring season (Fig. 5). Significant ($p < 0.05$) positive correlations were observed between the chronologies and temperatures (minimum and mean) in most months and seasons, except for the spring season. However, maximum temperature showed negative correlations with tree growth during spring months (Fig. 5). Similarly, significant positive correlations were found between the chronologies at low- to mid-elevations and precipitation during April and May. Additionally, correlations with spring season (MAM) total precipitation were significantly positive at elevations below 3850 m a.s.l. (Fig. 5). Significant positive correlations were detected between chronologies and SPEI03 for low to mid-elevations during the spring months from March to May (Fig. 5).

Seasonal climatic response confirmed that temperature is the primary limiting factor for the growth of *A. spectabilis* at all elevations (Fig. S3), with higher elevations being more affected. However, during spring, moisture availability also plays an important role in limiting tree growth at low- to mid-elevations (Fig. S3). The correlation between growth and spring season temperature and precipitation is stable over time (Fig. S4, S5), while the response with summer season temperature is consistently positive for the lower elevation sites but slightly different for the upper treeline (4100m) and timberline (3850m) sites. The response with winter precipitation is unstable, while the response with spring SPEI03 varies with elevation and is relatively stable at lower elevations for spring season but unstable for winter and summer seasons (Fig. S5).

3.3. Long-term growth trends

The BAI chronologies of *A. spectabilis* at low- to mid-elevations (3400–3800 m a.s.l.) have been decreasing in recent decades, while trees from the treeline (4100 m a.s.l.) and timberline (3850 m a.s.l.) have shown a growth increase (Fig. S6). The year 1980 was identified as the breakpoint for all sites, based on the density distribution of breakpoints in BAI residuals for the common period 1950–2011 (Fig. S7). Trend analyses of climate variables (Fig. S1) also showed a strong increase in temperatures after the 1980s. Growth trends were identified by fitting linear mixed-effects models on the GAMM detrended BAI residuals (Fig. 6, Fig. S8, Table S1), showing steady growth during 1950–1980 ($p > 0.05$), but a declining growth at middle and low elevations during 1981–2011 (Fig. 6c–e) and a strong positive trend at the treeline (4100 m a.s.l.) site (Fig. 6a). There was also a significant effect ($\beta = 0.009$, $p < 0.001$ during 1981–2011) of interaction between site and year as covariates (Table S2).

4. Discussion

4.1. Climatic sensitivity of fir growth

This study developed six tree-ring site chronologies of *A. spectabilis*

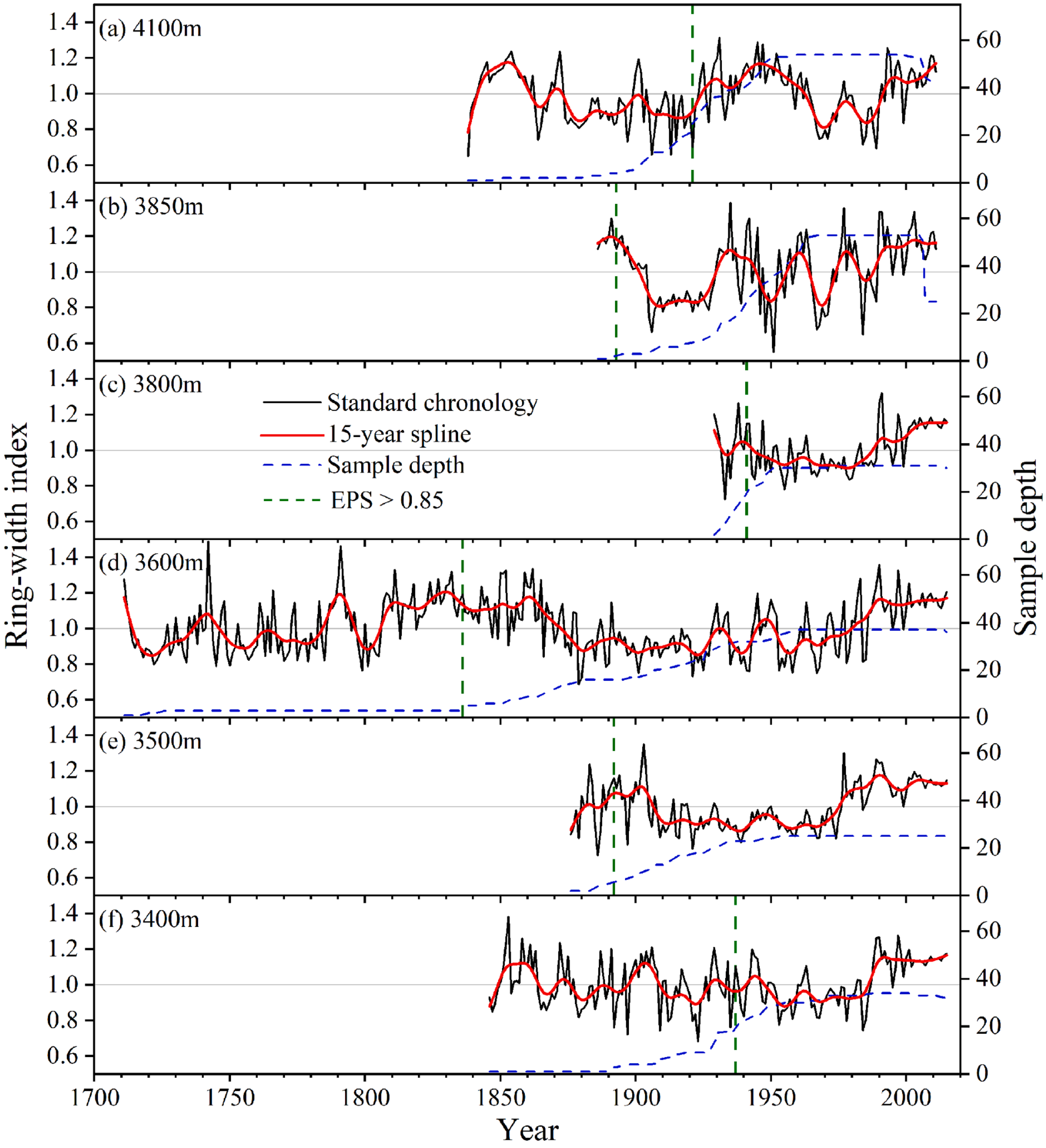

Fig. 3. Tree ring-width chronologies (black lines) of *Abies spectabilis* with sample depth (blue dashed line) along an elevation gradient in the Mt. Everest region of the central Himalaya: (a) 4100m, (b) 3850m, (c) 3800m, (d) 3600m, (e) 3500m, and (f) 3400m. A 15-year spline smoothing filter is denoted by the red line. The vertical green dashed line indicates the year after which expressed population signal (EPS) is greater than 0.85.

along an elevation gradient from 3400 to 4100 m a.s.l. in the Mt. Everest region of the central Himalaya. The chronologies' statistics (MS, SD, EPS, and Rbar) clearly underline their high dendroclimatic potential and represent the studied population at all elevation belts. The growth parameters (AGR, SD, and MS) generally declined with increasing elevation, while AC1, which indicates a carry-over effect from the previous year's growth (Fritts, 1976), increased (Table 1).

The PCA analysis showed that *A. spectabilis* chronologies captured a common climatic signal related to temperature change, with 65.7% variance explained by the first PC (Fig. 4a). Climate-growth analyses revealed that *A. spectabilis* growth along the elevation gradient is primarily limited by low temperatures during and proceeding the growth period, and secondarily by moisture availability during the spring season (Fig. 5). The positive relationship between growth and temperature during different seasons indicate a shift towards the critical temperature requirement for photosynthesis, xylogenesis, growth, and changing vegetation phenology (Rossi et al., 2008; Li et al., 2017; Yang et al., 2017). The strong relationship between the chronologies and winter temperature may indicate a chilling requirement of the trees in temperate or cold climatic regions above 3,000 m a.s.l. (Luedeling et al., 2011; Guo et al., 2014). Increasing winter temperatures facilitate early snow melting, providing additional meltwater for growth during the early growing season in spring. Similarly, higher winter temperatures prevent deep soil freezing, ice crystal formation, and other mechanical injuries (Shah et al., 2019; Gaire et al., 2020; Panthi et al., 2020). Winter cold may induce root damage (Tierney et al., 2001; Reinmann et al., 2019) or major delay of bud burst (Rotzer et al., 2004; Basler and Korner, 2014), ultimately reducing tree growth (Weigel et al., 2018;

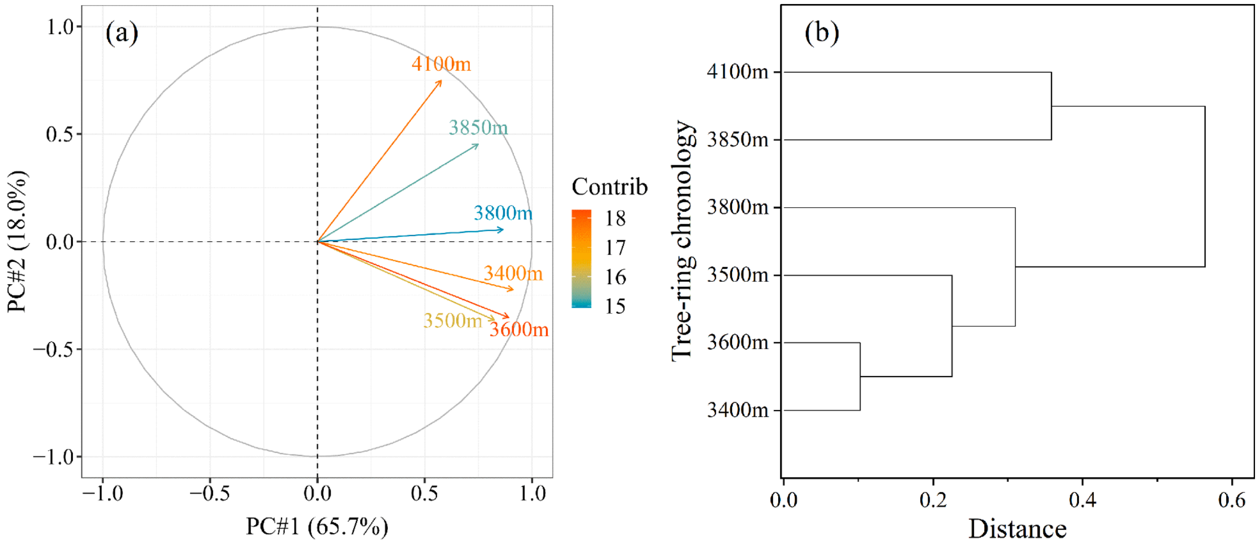

Fig. 4. Principal component analysis (a) and cluster dendrogram (b) of *Abies spectabilis* ring-width chronologies from different elevation belts in the Mt. Everest region.

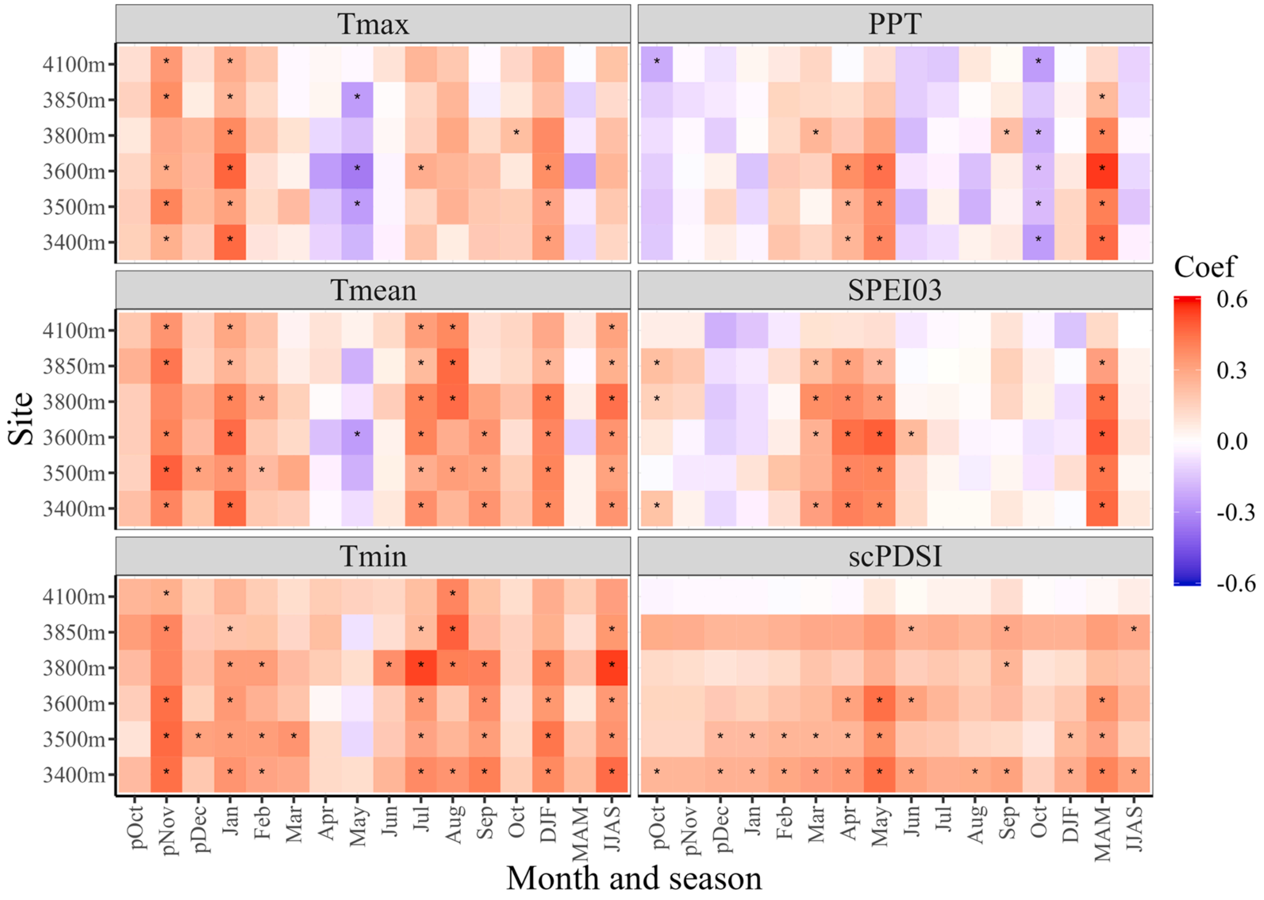

Fig. 5. Correlogram showing the relationships (Pearson's correlation coefficient) between climate and six ring-width chronologies of *Abies spectabilis* from the Mt. Everest region. Tmax, Tmean, Tmin, PPT, SPEI03, and scPDSI indicate maximum temperature, mean temperature, minimum temperature, precipitation, three-month standardized precipitation-evapotranspiration index, and self-calibrated Palmer drought severity index, respectively. Seasons: winter (DJF), spring (MAM), and summer (JJAS) were used for analyzing seasonal responses. The significant correlation ($p < 0.05$) is indicated by an asterisk.

Harvey et al., 2019). The positive growth response to winter temperatures at high-elevation sites is a common response shared with other species, including *A. spectabilis, A. pindrow, Cedrus deodara*, and *Pinus wallichiana* in the central and western Himalaya (Cook et al., 2003; Chhetri and Cairns, 2016; Shrestha et al., 2017; Sohar et al., 2017; Shah et al., 2019; Gaire et al., 2020). Moreover, increasing summer temperatures were found to have a positive effect on tree growth. The Himalayan region is warm and moist, receiving approximately 80% of its

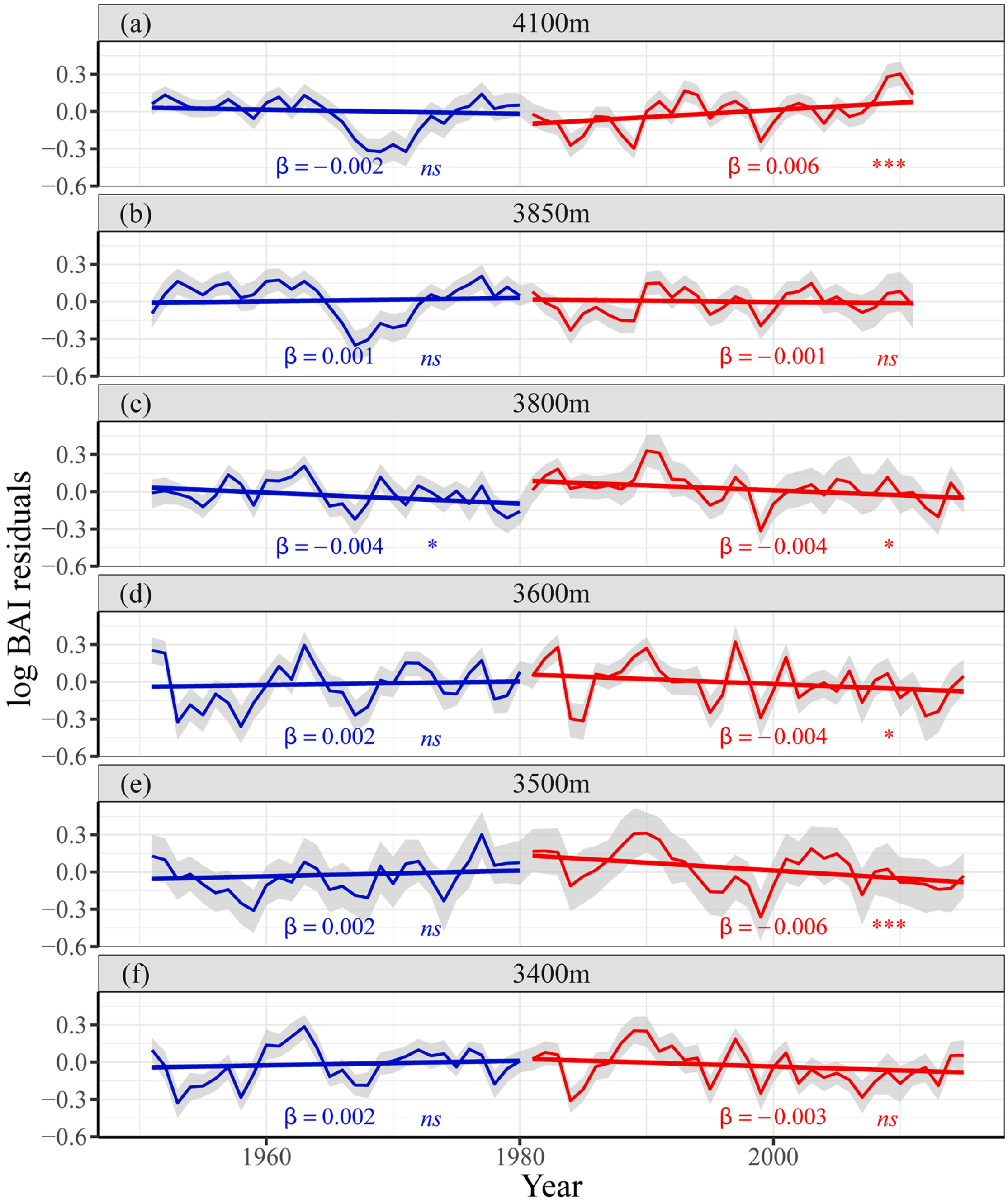

Fig. 6. Long-term trends in tree growth (log BAI residuals) of *Abies spectabilis* along an elevation gradient in the Mt. Everest region, the central Himalaya for the common period 1950–2011: (a) 4100m, (b) 3850m, (c) 3800m, (d) 3600m, (e) 3500m, and (f) 3400m. The trend is presented in two subperiods i.e. 1950–1980 (blue) and 1981–2011 (red). The grey shaded area represents 95% confidence interval.

annual rainfall (DHM, 2017). Similarly, other conifers from the Himalaya have also shown positive growth responses to temperature during both winter and summer (Chhetri and Cairns, 2016; Shrestha et al., 2017; Gaire et al., 2017, 2020; Schwab et al., 2018). Consistent with our study, positive responses to summer temperature were observed for many treelines and high-elevation sites in the central Himalaya (Lv and Zhang, 2012; Chhetri and Cairns, 2016; Gaire et al., 2017; Shrestha et al., 2017; Schwab et al., 2018).

Spring season climate has a significant influence on fir growth with positive relationships between fir growth and total precipitation, as well as SPEI03 during spring months and season in all elevations, although not significant at the upper treeline (Fig. 5). Negative relationships were found between Himalayan silver fir chronologies and mean and maximum temperatures during late spring months (April–May) in most elevations, indicating that moisture availability or temperature-induced drought stress prevails during the mid- to late-spring season before the onset of the wet summer monsoon season, especially at low- to mid-elevation belts. The study region receives little or even no rainfall during spring (Salerno et al., 2015; DHM, 2017; Talchabhadel et al., 2018), and increasing temperatures enhance evapotranspiration demands and create moisture stress, ultimately limiting tree growth (Liang et al., 2014; Panthi et al., 2020). Therefore, a very hot spring season without sufficient moisture was found to be detrimental to tree growth, especially for fir trees growing at the low- to mid-elevations. The potential evapotranspiration in the Himalaya reaches a maximum during the pre-monsoon season in April–May, but this effect likely plays a minor role at high elevations due to the rapid decrease in evapotranspiration with elevation (Lambert and Chitrakar, 1989). Trees at the treeline and timberline could get more water from soil recharged with meltwater from higher elevations. Higher elevation sites are less affected by evaporative water loss due to lower temperature, making them less vulnerable to moisture stress compared to the trees at lower elevation belts. This explains why we found strong positive relations with spring precipitation at low elevations and why the importance of moisture stress during the spring season decreased with increasing elevations.

Partial correlation analysis revealed that the importance of temperature for tree growth increases with elevation, while the importance of moisture availability during spring is higher at low elevations. A previous study found that radial growth of *A. spectabilis* in lower elevation sites was significantly positively correlated with PDSI from the previous September to the current September, while at the upper elevation belt, the response with PDSI was weak and more related to temperature (Lv and Zhang, 2012). Similar to them, our study found positive relationships between tree growth and SPEI03 during spring at low- to mid-elevations and also positive relationships between the chronologies from low- to mid-elevations and scPDSI in almost all months of the year (Fig. 5). The similarity in the response of fir growth in both the northern and southern declivity of Mt. Everest indicated that in both areas they are more sensitive to moisture stress at low- to mid-elevations, while they are more sensitive to temperature at high elevations. Hence, fir could act as an indicator of climate change impacts on forests in broader areas. This also implies that trees growing in the high-elevation inner valleys in the Himalaya are not only sensitive to temperature change but also vulnerable to moisture stress. The positive relationship between temperature and tree growth at the treeline and the timberline suggests a potential range expansion of Himalayan silver fir. A previous study in Langtang reported that *A. spectabilis* can compete and replace the treeline-associated *Rhododendron campanulatum* and move upward (Mainali et al., 2020). Analyses of more than 70 chronologies of *A. spectabilis* covering its entire distribution range in the Himalaya (Gaire et al., 2020) revealed a site-specific growth trend and broader (spring season signal) to site-specific climatic responses, depending on the climatic regimes of the sampling site (Gaire et al., 2015).

4.2. *Temporal stability of the growth-climate response*

Moving correlations revealed that growth responses to spring season temperature, precipitation, and SPEI03 remain almost similar throughout analyzing period from 1951 to 2011 (Fig. S5). The importance of winter temperatures (mean and minimum) for tree growth has been weakening during recent years at lower elevations, while at higher elevations, its importance is increasing. The importance of spring season precipitation is enhanced at lower elevations (Fig. S5). The negative relationship with the spring season mean temperature became stronger at low- to mid-elevation belts. However, the response to summer season precipitation is changing over time and varies along elevation, while the response to summer season SPEI03 is stable over time and along elevation. Previous studies on the temporal climatic responses of the trees from the Himalaya have shown similar stable to changing growth-climate responses over time (Yadav et al., 2004; Sohar et al., 2017; Schwab et al., 2018; Gaire et al., 2020). Comparing the findings of moving responses among studies, it can be inferred that the climatic response of tree species in the Himalaya can be temporally stable or changing, highly depending on the investigated species and local site conditions. Such temporally stable to changing climatic responses of tree species are also observed in the Tibetan Plateau adjacent to the Himalaya (Zhang and Wilmking, 2010; Dang et al., 2013; Yu et al., 2013; Zhang et al., 2017).

4.3. *Long-term trends of tree growth*

All six ring-width chronologies of *A. spectabilis* in the Mt. Everest region have shown positive growth trends since the second half of the 20th century (Fig. 3), which can be linked to an overall temperature increase in the high Himalaya during the last century (Salerno et al., 2015; Thakuri et al., 2019). However, ring-width chronologies from middle and low elevations have shown a negative growth trend during the most recent one to two decades (Fig. 3c–f), possibly due to an intensified spring season drought (Liang et al., 2019). Similarly, negative growth trends were reported at lower elevation sites, while positive growth trends were detected at high elevations in western Nepal, central Himalaya (Gaire et al., 2020; Panthi et al., 2020). Differences in short- or medium-term growth trends among the chronologies could be caused by variations in micro-topography, slopes, aspects, and micro-climatic conditions (Babushkina et al., 2018; Liu et al., 2018). Previous studies from the Himalayan region have indicated both, increasing and decreasing growth trends during the 20th century, depending on the site and dominant climate regime (Kharal et al., 2017; Shrestha et al., 2017; Rai et al., 2019; Gaire et al., 2020; Panthi et al., 2020). In some Himalayan sites (Langtang, Mustang, and Manang), no single persistent growth trend was observed throughout the elevation gradient during the 20th century (Kharal et al., 2017; Shrestha et al., 2017; Rai et al., 2019). Previous studies from the Mt. Everest region have revealed an increasing greening and invasion of plants into the sub-nival belt (Anderson et al., 2020), stand densification, and/or upward treeline shifting (Gaire et al., 2017; Sigdel et al., 2018). The positive growth trend in response to climate change in areas, especially at treeline and timberline belts, indicates a trend towards further growth enhancement and probable range shift of the investigated species.

Long-term growth trend analyses detected decreasing trends at low- to mid-elevation sites but a strong increasing trend at the treeline (4100 m a.s.l.) during recent decades (1981–2011) while no obvious trends were found at all sites during the period (1951–1980) (Fig. 6). The decreasing growth trends at low- to mid-elevation sites in the Himalayan region may be related to recent intensified drought conditions during the spring season (Tiwari et al., 2017; Liang et al., 2019). Moreover, growth decline may also associate with warming-induced drought stress (Körner, 2015; Tiwari et al., 2017; Gao et al., 2020). Ren et al. (2018) reported that moisture deficits during the spring season may prolong the cambial dormancy, which may limit the start of cambial activity and tree radial growth. Similarly, *A. delavayi* in the Cangshan Mountains, southwestern China, also showed decreasing growth trend since the 1950s, attributed to the increased temperature and decreased moisture availability (Yang et al., 2022). Besides, the recent declining growth trends were also found in Tibetan Plateau (Liang et al., 2016) and Himalayan regions (Panthi et al., 2020). However, for the high elevation site (treeline at 4100 m a.s.l.) in Mt. Everest, *A. spectabilis* may likely benefit from the warming climate induced by significant rising temperatures after the 1980s (Fig. S1), which may accelerate photosynthesis, ultimately enhanced tree growth (Salerno et al., 2015; Thakuri et al., 2019).

5. Conclusions

We developed six tree ring-width chronologies of *A. spectabilis* along an elevation gradient in the Mt. Everest region, the central Himalaya. The climate response of Himalayan silver fir along an elevation gradient in the Mt. Everest region indicates that temperature during and preceding the growing season is the primary limiting factor for growth, with moisture availability during spring being the second relevant growth factor, especially in lower-elevation forest belts. Positive growth trend at the treeline site over the recent decades likely relates to the effect of the warming climate. Negative growth trends at low- to mid-elevation belts may relate to recent intensified drought conditions during the spring season. These findings highlight the importance of focusing more on the middle and low elevations as increased warming (since the 1980s) induces growth declines, which is an early warning of forest vulnerability to future climate change. Further investigations on cambial activity, daily/seasonal stem diameter variations, and sap-flow measurements on multiple tree species in the Himalayan region may bring a comprehensive understanding of tree physiological processes to the warming climate and changing environmental conditions.

Declaration of Competing Interest

The authors declare that they have no known competing financial interests or personal relationships that could have appeared to influence the work reported in this paper.

Data availability

Data will be made available on request.

Acknowledgments

This study was funded by the National Natural Science Foundation of China (NSFC, 31861133007, 31770533) and EvK2CNR-Italy. NPG and ZZ were supported by the CAS-PIFI post-doctoral fellowship (2019PC0102) and the XTBG post-doctoral fellowship (279734), respectively. ZXF was also supported by the Ten Thousand Talent Project of Yunnan Province (YNWR-QNBJ-2019-190) and by the West Light Talent Program of the Chinese Academy of Sciences (xbzg-zdsys-202218). We thank DNPWC-Nepal for research permission, DHM-Nepal for meteorological and hydrological data, and local field assistants for their support during tree-ring sampling.

Supplementary materials

Supplementary material associated with this article can be found, in the online version, at doi:10.1016/j.agrformet.2023.109575.

References

Agarwal, A., Babel, M.S., Maskey, S., Shrestha, S., Kawasaki, A., Tripathi, N.K., 2016. Analysis of temperature projections in the Koshi River Basin, Nepal. Int. J. Climatol. 36 (1), 266–279. https://doi.org/10.1002/joc.4342.

Anderson, K., Fawcett, D., Cugulliere, A., Benford, S., Jones, D., Leng, R.L., 2020. Vegetation expansion in the subnival Hindu Kush Himalaya. Glob. Change Biol. 26 (3), 1608–1625. https://doi.org/10.1111/gcb.14919.

Babst, F., Bouriaud, O., Poulter, B., Trouet, V., Girardin, M.P., Frank, D.C., 2019. Twentieth century redistribution in climatic drivers of global tree growth. Sci. Adv. 5 (1), eaat4313. https://doi.org/10.1126/sciadv.aat4313.

Babushkina, E., Belokopytova, L., Zhirnova, D., Barabantsova, A., Vaganov, E., 2018. Divergent growth trends and climatic response of *Picea obovata* along elevational gradient in Western Sayan mountains, Siberia. J. Mt. Sci. 15 (11), 2378–2397. https://doi.org/10.1007/s11629-018-4974-6.

Basler, D., Korner, C., 2014. Photoperiod and temperature responses of bud swelling and bud burst in four temperate forest tree species. Tree Physiol. 34 (4), 377–388. https://doi.org/10.1093/treephys/tpu021.

Benn, D.I., Bolch, T., Hands, K., Gulley, J., Luckman, A., Nicholson, L.I., Wiseman, S., 2012. Response of debris-covered glaciers in the Mount Everest region to recent warming, and implications for outburst flood hazards. Earth Sci. Rev. 114 (1–2), 156–174. https://doi.org/10.1016/j.earscirev.2012.03.008.

Brandt, J.S., Haynes, M.A., Kuemmerle, T., Waller, D.M., Radeloff, V.C., 2013. Regime shift on the roof of the world: Alpine meadows converting to shrublands in the southern Himalayas. Biol. Conserv. 158, 116–127. https://doi.org/10.1016/j.biocon.2012.07.026.

Briffa, K.R., 1995. Interpreting high-resolution proxy climate data, the example of dendroclimatology. In: von Storch, H., Navarra, A. (Eds.), Analysis of Climate Data Variability, Applications of Statistical Techniques. Springer, New York, pp. 77–94.

Bunn, A.G., 2008. A dendrochronology program library in R (dplR). Dendrochronologia 26 (2), 115–124. https://doi.org/10.1016/j.dendro.2008.01.002.

Byers, A.C., 2007. Changing climates, changing lives: strengthening adaptive response capacities to climate change in the Huascarán Biosphere Reserve, Peru, and Sagarmatha (Mt. Everest) National Park, Nepal. Dev. Earth Surf. Process. 10, 249–250. https://doi.org/10.1016/S0928-2025(06)10027-9.

Chhetri, P.K., Cairns, D.M., 2016. Dendroclimatic response of *Abies spectabilis* at treeline ecotone of Barun Valley, eastern Nepal Himalaya. J. For. Res. 27 (5), 1163–1170. https://doi.org/10.1007/s11676-016-0249-7.

Cook, E.R., Krusic, P.J., Jones, P.D., 2003. Dendroclimatic signals in long tree-ring chronologies from the Himalayas of Nepal. Int. J. Climatol. 23 (7), 707–732. https://doi.org/10.1002/joc.911.

Dang, H., Zhang, Y., Zhang, K., Jiang, M., Zhang, Q., 2013. Climate-growth relationships of subalpine fir (*Abies fargesii*) across the altitudinal range in the Shennongjia Mountains, central China. Clim. Change 117 (4), 903–917. https://doi.org/10.1007/s10584-012-0611-5.

de Vries, A. & Ripley, B. D. (2022). ggdendro: create dendrograms and tree diagrams using ‘ggplot2’. R package version 0.1.23. https://CRAN.R-project.org/package=ggdendro.

DHM, 2017. Study of climate and climatic variation over Nepal. Department of Hydrology and Meteorology, Ministry of Science, Technology and Environment, Government of Nepal, Kathmandu, Nepal.

DNPWC, 2015. In: Dhakal, M. (Ed.), Protected Areas of Nepal. Department of National Park and Wildlife Conservation, Babarmal, Kathmandu, Nepal.

Dolezal, J., Dvorsky, M., Kopecky, M., Liancourt, P., Hiiesalu, I., Macek, M., Schweingruber, F., 2016. Vegetation dynamics at the upper elevational limit of vascular plants in Himalaya. Sci. Rep. 6 (1), 24881. https://doi.org/10.1038/srep24881.

Fan, Z.-X., Bräuning, A., Cao, K.-F., Zhu, S.-D., 2009. Growth–climate responses of high-elevation conifers in the central Hengduan Mountains, southwestern China. For. Ecol. Manag. 258 (3), 306–313. https://doi.org/10.1016/j.foreco.2009.04.017.

Ferrarini, A., Rossi, G., Mondoni, A., Orsenigo, S., 2014. Prediction of climate warming impacts on plant species could be more complex than expected. Evidence from a case study in the Himalaya. Ecol. Compl. 20, 307–314. https://doi.org/10.1016/j.ecocom.2014.02.003.

Fritts, H.C., 1976. Tree Rings and Climate. Academic Press, New York, San Francisco.

Fukui, K., Fujii, Y., Ageta, Y., Asahi, K., 2007. Changes in the lower limit of mountain permafrost between 1973 and 2004 in the Khumbu Himal, the Nepal Himalayas. Glob. Planet. Change 55 (4), 251–256. https://doi.org/10.1016/j.gloplacha.2006.06.002.

Gaire, N.P., Dhakal, Y.R., Shah, S.K., Fan, Z.-X., Bräuning, A., Thapa, U.K., Bhuju, D.R., 2019. Drought (scPDSI) reconstruction of trans-Himalayan region of central Himalaya using *Pinus wallichiana* tree-rings. Palaeogeogr. Palaeoclimatol. Palaeoecol. 514, 251–264. https://doi.org/10.1016/j.palaeo.2018.10.026.

Gaire, N.P., Fan, Z.-X., Bräuning, A., Panthi, S., Rana, P., Shrestha, A., Bhuju, D.R., 2020. *Abies spectabilis* shows stable growth relations to temperature, but changing response to moisture conditions along an elevation gradient in the central Himalaya. Dendrochronologia 60, 125675. https://doi.org/10.1016/j.dendro.2020.125675.

Gaire, N.P., Koirala, M., Bhuju, D.R., Carrer, M., 2017. Site- and species-specific treeline responses to climatic variability in eastern Nepal Himalaya. Dendrochronologia 41, 44–56. https://doi.org/10.1016/j.dendro.2016.03.001.

Gaire, N.P., Rana, P., Koirala, M., Bhuju, D.R., Carrer, M., 2015. Study of treeline ecotone to assess long-term impact of environmental change in Mt. Everest region, Nepal Himalaya. FUUAST J. Biol. 5 (1), 1–11.

Gaire, N.P., Zaw, Z., Bräuning, A., Sharma, B., Raj Dhakal, Y., Timilsena, R., Fan, Z-X., 2022. Increasing extreme events in the central Himalaya revealed from a tree-ring based multi-century streamflow reconstruction of Karnali River Basin. J. Hydrol. 610, 127801 https://doi.org/10.1016/j.jhydrol.2022.127801.

Gao, L., Gou, X., Deng, Y., Liu, W., Yang, M., Zhao, Z., 2013. Climate–growth analysis of *Qilian juniper* across an altitudinal gradient in the central Qilian Mountains, northwest China. Trees 27 (2), 379–388. https://doi.org/10.1007/s00468-012-0776-6.

Gao, S., Wang, Y., Yu, S., Huang, Y., Liu, H., Chen, W., He, X., 2020. Effects of drought stress on growth, physiology and secondary metabolites of Two Adonis species in Northeast China. Sci. Hortic. 259, 108795 https://doi.org/10.1016/j.scienta.2019.108795.

Gonzalez, P., Neilson, R.P., Lenihan, J.M., Drapek, R.J., 2010. Global patterns in the vulnerability of ecosystems to vegetation shifts due to climate change. Glob. Ecol. Biogeogr. 19 (6), 755–768. https://doi.org/10.1111/j.1466-8238.2010.00558.x.

Guo, L., Dai, J., Ranjitkar, S., Yu, H., Xu, J., Luedeling, E., 2014. Chilling and heat requirements for flowering in temperate fruit trees. Int. J. Biometeorol. 58 (6), 1195–1206. https://doi.org/10.1007/s00484-013-0714-3.

Harris, I., Osborn, T.J., Jones, P., Lister, D., 2020. Version 4 of the CRU TS monthly high-resolution gridded multivariate climate dataset. Sci. Data 7 (1), 1–18. https://doi.org/10.1038/s41597-020-0453-3.

Harvey, J.E., Smiljanic, M., Scharnweber, T., Buras, A., Cedro, A., Cruz-Garcia, R., Wilmking, M., 2019. Tree growth influenced by warming winter climate and summer moisture availability in northern temperate forests. Glob. Change Biol. 26, 2505–2518. https://doi.org/10.1111/gcb.14966.

Holmes, R.L., 1983. Computer-assisted quality control in tree-ring dating and measurement. Tree-Ring Bull. 43, 69–78.

IPCC, 2014. In: Barros, V.R., Field, C.B., Dokken, D.J., Mastrandrea, M.D., Mach, K.J., Bilir, T.E., Chatterjee, M., Ebi, K.L., Estrada, Y.O., Genova, R.C., Girma, B., Kissel, E. S., Levy, A.N., MacCracken, S., Mastrandrea, P.R., White, L.L. (Eds.), Climate change 2014: Impacts, adaptation, and vulnerability. Part B: Regional aspects. Contribution of working group II to the fifth assessment report of the intergovernmental panel on climate change. Cambridge University Press, Cambridge, United Kingdom, p. 688.

IPCC, 2022. In: Pörtner, H.O., Roberts, D.C., Tignor, M., Poloczanska, E.S., Mintenbeck, K., Alegría, A., Craig, M., Langsdorf, S., Löschke, S., Möller, V., Okem, A., Rama, B. (Eds.), Climate change 2022: Impacts, adaptation, and vulnerability. Contribution of working group II to the sixth assessment report of the intergovernmental panel on climate change. Cambridge University Press, Cambridge, UK and New York, NY, USA, p. 3056. Cambridge University Press.

Jha, P.K., 2010. An overview of Sagarmatha (Mt. Everest) region, Nepal. In: Jha, P.K., Khanal, I.P. (Eds.), Contemporary Research in Sagarmatha (Mt. Everest) Region, Nepal. Nepal Academy of Science and Technology, Khumaltar, Lalitpur, pp. 1–14.

Karki, R., ul Hasson, S., Gerlitz, L., Talchabhadel, R., Schickhoff, U., Scholten, T., Bohner, J., 2020. Rising mean and extreme near-surface air temperature across Nepal. Int. J. Climatol. 40 (4), 2445–2463. https://doi.org/10.1002/joc.6344.

Kharal, D.K., Meilby, H., Rayamajhi, S., Bhuju, D., Thapa, U.K., 2014. Tree ring variability and climate response of *Abies spectabilis* along an elevation gradient in Mustang, Nepal. Banko Janakari 24, 3–13. https://doi.org/10.3126/banko.v24i1.13473.

Kharal, D.K., Thapa, U.K., St George, S., Meilby, H., Rayamajhi, S., Bhuju, D.R, 2017. Tree-climate relations along an elevational transect in Manang Valley, central Nepal. Dendrochronologia 41, 57–64. https://doi.org/10.1016/j.dendro.2016.04.004.

Körner, C., 2012. Alpine Treelines: Functional Ecology Of The Global High Elevation Tree Limits. Springer.

Körner, C., 2015. Paradigm shift in plant growth control. Curr. Opin. Plant Biol. 25, 107–114. https://doi.org/10.1016/j.pbi.2015.05.003.

Lambert, L., Chitrakar, B.D., 1989. Variation of potential evapotranspiration with elevation in Nepal. Mt. Res. Dev. 9 (2), 145–152. https://doi.org/10.2307/3673477.

Lê, S., Josse, J., Husson, F., 2008. FactoMineR: An R package for multivariate analysis. J. Stat. Softw. 25 (1), 1–18. https://doi.org/10.18637/jss.v025.i01.

Leblanc, D.C., 1990. Relationships between breast-height and whole-stem growth indexes for red spruce on whiteface mountain, New York. Can. J. For. Res. 20 (9), 1399–1407. https://doi.org/10.1139/x90-185.

Li, X., Liang, E., Gričar, J., Rossi, S., Čufar, K., Ellison, A.M., 2017. Critical minimum temperature limits xylogenesis and maintains treelines on the southeastern Tibetan Plateau. Sci. Bull. 62 (11), 804–812. https://doi.org/10.1016/j.scib.2017.04.025.

Liang, E.Y., Dawadi, B., Pederson, N., Eckstein, D., 2014. Is the growth of birch at the upper timberline in the Himalayas limited by moisture or by temperature? Ecology 95, 2453–2465. https://doi.org/10.1890/13-1904.1.

Liang, E., Dawadi, B., Pederson, N., Piao, S., Zhu, H., Sigdel, S.R., Chen, D., 2019. Strong link between large tropical volcanic eruptions and severe droughts prior to monsoon in the central Himalayas revealed by tree-ring records. Sci. Bull. 64 (14), 1018–1023. https://doi.org/10.1016/j.scib.2019.05.002.

Liang, E., Leuschner, C., Dulamsuren, C., Wagner, B., Hauck, M., 2016. Global warming-related tree growth decline and mortality on the north-eastern Tibetan plateau. Clim. Change 134 (1–2), 163–176. https://doi.org/10.1007/s10584-015-1531-y.

Liang, E., Wang, Y., Xu, Y., Liu, B., Shao, X., 2010. Growth variation in *Abies georgei* var. smithii along altitudinal gradients in the Sygera Mountains, southeastern Tibetan Plateau. Trees 24 (2), 363–373. https://doi.org/10.1007/s00468-009-0406-0.

Liu, B., Liang, E., Liu, K., Camarero, J., 2018. Species- and elevation-dependent growth responses to climate warming of Mountain forests in the Qinling Mountains, central China. Forests 9 (5), 248. https://doi.org/10.3390/f9050248.

Liu, X., Cheng, Z., Yan, L., Yin, Z.-Y., 2009. Elevation dependency of recent and future minimum surface air temperature trends in the Tibetan Plateau and its surroundings. Glob. Planet. Change 68 (3), 164–174. https://doi.org/10.1016/j.gloplacha.2009.03.017.

Luedeling, E., Girvetz, E.H., Semenov, M.A., Brown, P.H., 2011. Climate change affects winter chill for temperate fruit and nut trees. PLoS One 6 (5), e20155. https://doi.org/10.1371/journal.pone.0020155.

Lv, L.X., Zhang, Q.B., 2012. Asynchronous recruitment history of *Abies spectabilis* along an altitudinal gradient in the Mt. Everest region. J. Plant Ecol. 5 (2), 147–156. https://doi.org/10.1093/jpe/rtr016.

Lyu, L., Deng, X., Zhang, Q.B., 2016. Elevation pattern in growth coherency on the southeastern Tibetan Plateau. PLoS One 11 (9), e0163201. https://doi.org/10.1371/journal.pone.0163201.

Mainali, K., Shrestha, B.B., Sharma, R.K., Adhikari, A., Gurarie, E., Singer, M., Parmesan, C., 2020. Contrasting responses to climate change at Himalayan treelines revealed by population demographics of two dominant species. Ecol. Evol. 10 (3), 1209–1222. https://doi.org/10.1002/ece3.5968.

Melvin, T.M., Briffa, K.R., 2008. A "signal-free" approach to dendroclimatic standardisation. Dendrochronologia 26 (2), 71–86. https://doi.org/10.1016/j.dendro.2007.12.001.

Muggeo, V.M.R., 2017. Interval estimation for the breakpoint in segmented regression: a smoothed score-based approach. Aust. N. Z. J. Stat. 59 (3), 311–322. https://doi.org/10.1111/anzs.12200.

Panthi, S., Fan, Z.X., van der Sleen, P., Zuidema, P.A., 2020. Long-term physiological and growth responses of Himalayan fir to environmental change are mediated by mean climate. Glob. Change Biol. 26 (3), 1778–1794. https://doi.org/10.1111/gcb.14910.

Phipps, R.L., Whiton, J.C., 1988. Decline in long-term growth trends of white oak. Can. J. For. Res. 18 (1), 24–32. https://doi.org/10.1139/x88-005.

Pinheiro, J., Bates, D., DebRoy, S., & Sarkar, D. (2021). The R core team nlme: linear and nonlinear mixed effects models. R. package version, 3, 1–152. https://CRAN.R-project.org/package=nlme.

Qi, W., Zhang, Y., Gao, J., Yang, X., Liu, L., Khanal, N.R., 2013. Climate change on the southern slope of Mt. Qomolangma (Everest) Region in Nepal since 1971. J. Geog. Sci. 23 (4), 595–611. https://doi.org/10.1007/s11442-013-1031-9.

Rai, S., Dawadi, B., Wang, Y., Lu, X., Ru, H., Sigdel, S.R., 2019. Growth response of *Abies spectabilis* to climate along an elevation gradient of the Manang valley in the central Himalayas. J. For. Res. 31 (6), 2245–2254. https://doi.org/10.1007/s11676-019-01011-x.

Reinmann, A.B., Susser, J.R., Demaria, E.M.C., Templer, P.H., 2019. Declines in northern forest tree growth following snowpack decline and soil freezing. Glob. Change Biol. 25 (2), 420–430. https://doi.org/10.1111/gcb.14420.

Ren, P., Rossi, S., Camarero, J.J., Ellison, A.M., Liang, E., Penuelas, J., 2018. Critical temperature and precipitation thresholds for the onset of xylogenesis of *Juniperus przewalskii* in a semi-arid area of the north-eastern Tibetan Plateau. Ann. Bot. 121 (4), 617–624. https://doi.org/10.1093/aob/mcx188.

Rinn, F. (2010). TSAP-Win: time series analysis and presentation for dendrochronology and related applications. Version 0.55 User reference. Heidelberg, Germany.

Rossi, S., Deslauriers, A., Griçar, J., Seo, J.-W., Rathgeber, C.B.K., Anfodillo, T., Jalkanen, R., 2008. Critical temperatures for xylogenesis in conifers of cold climates. Glob. Ecol. Biogeogr. 17 (6), 696–707. https://doi.org/10.1111/j.1466-8238.2008.00417.x.

Rotzer, T., Grote, R., Pretzsch, H., 2004. The timing of bud burst and its effect on tree growth. Int. J. Biometeorol. 48 (3), 109–118. https://doi.org/10.1007/s00484-003-0191-1.

Salerno, F., Guyennon, N., Thakuri, S., Viviano, G., Romano, E., Vuillermoz, E., Tartari, G., 2015. Weak precipitation, warm winters and springs impact glaciers of south slopes of Mt. Everest (central Himalaya) in the last 2 decades (1994–2013). Cryosphere 9 (3), 1229–1247. https://doi.org/10.5194/tc-9-1229-2015.

Schwab, N., Kaczka, R., Janecka, K., Böhner, J., Chaudhary, R., Scholten, T., Schickhoff, U., 2018. Climate change-induced shift of tree growth sensitivity at a central Himalayan treeline ecotone. Forests 9 (5), 267. https://doi.org/10.3390/f9050267.

Shah, S.K., Pandey, U., Mehrotra, N., Wiles, G.C., Chandra, R., 2019. A winter temperature reconstruction for the Lidder Valley, Kashmir, Northwest Himalaya based on tree-rings of *Pinus wallichiana*. Clim. Dyn. 53 (7–8), 4059–4075. https://doi.org/10.1007/s00382-019-04773-6.

Shrestha, B.B., Jha, P.K., 2010. Rhododendrons in Sagarmatha National Park, Nepal. In: Jha, P.K., Khanal, I.P. (Eds.), Contemporary Research in Sagarmatha (Mt. Everest) Region, Nepal. Nepal Academy of Science and Technology, Khumaltar, Lalitpur, pp. 189–198.

Shrestha, K.B., Chhetri, P.K., Bista, R., 2017. Growth responses of *Abies spectabilis* to climate variations along an elevational gradient in Langtang National Park in the central Himalaya, Nepal. J. For. Res. 22 (5), 274–281. https://doi.org/10.1080/13416979.2017.1351508.

Shrestha, K.B., Hofgaard, A., Vandvik, V., 2015. Recent treeline dynamics are similar between dry and mesic areas of Nepal, central Himalaya. J. Plant Ecol. 8 (4), 347–358. https://doi.org/10.1093/jpe/rtu035.

Shrestha, U.B., Gautam, S., Bawa, K.S., 2012. Widespread climate change in the Himalayas and associated changes in local ecosystems. PLoS One 7 (5), e36741. https://doi.org/10.1371/journal.pone.0036741.

Sigdel, S.R., Wang, Y., Camarero, J.J., Zhu, H., Liang, E., Penuelas, J., 2018. Moisture-mediated responsiveness of treeline shifts to global warming in the Himalayas. Glob. Change Biol. 24 (11), 5549–5559. https://doi.org/10.1111/gcb.14428.

Sohar, K., Altman, J., Lehečková, E., Doležal, J., 2017. Growth-climate relationships of Himalayan conifers along elevational and latitudinal gradients. Int. J. Climatol. 37 (5), 2593–2605. https://doi.org/10.1002/joc.4867.

Speer, J.H., 2010. Fundamentals of Tree-Ring Research. University of Arizona Press, Tucson, Arizona, p. 368. ISBN: 978-0-816-52684-0.

Sun, X.-B., Ren, G.-Y., Shrestha, A.B., Ren, Y.-Y., You, Q.-L., Zhan, Y.-J., Rajbhandari, R., 2017. Changes in extreme temperature events over the Hindu Kush Himalaya during 1961–2015. Adv. Clim. Change Res. 8 (3), 157–165. https://doi.org/10.1016/j.accre.2017.07.001.

Talchabhadel, R., Karki, R., Thapa, B.R., Maharjan, M., Parajuli, B., 2018. Spatio-temporal variability of extreme precipitation in Nepal. Int. J. Climatol. 38 (11), 4296–4313. https://doi.org/10.1002/joc.5669.

Talchabhadel, R., Karki, R., Yadav, M., Maharjan, M., Aryal, A., Thapa, B.R., 2019. Spatial distribution of soil moisture index across Nepal: A step towards sharing climatic information for agricultural sector. Theor. Appl. Climatol. 137 (3–4), 3089–3102. https://doi.org/10.1007/s00704-019-02801-3.

Telwala, Y., Brook, B.W., Manish, K., Pandit, M.K., 2013. Climate-induced elevational range shifts and increase in plant species richness in a Himalayan biodiversity epicentre. PLoS One 8 (2), e57103. https://doi.org/10.1371/journal.pone.0057103.

Thakuri, S., Dahal, S., Shrestha, D., Guyennon, N., Romano, E., Colombo, N., Salerno, F., 2019. Elevation-dependent warming of maximum air temperature in Nepal during 1976–2015. Atmos. Res. 228, 261–269. https://doi.org/10.1016/j.atmosres.2019.06.006.

Thakuri, S., Salerno, F., Smiraglia, C., Bolch, T., D'Agata, C., Viviano, G., Tartari, G., 2014. Tracing glacier changes since the 1960s on the south slope of Mt. Everest (central Southern Himalaya) using optical satellite imagery. Cryosphere 8 (4), 1297–1315. https://doi.org/10.5194/tc-8-1297-2014.

Tierney, G.L., Fahey, T.J., Peter, M., Hardy, J.P., Fitzhugh, R.D., Driscoll, C.T., 2001. Soil freezing alters fine root dynamics in a northern hardwood forest. Biogeochemistry 56, 175–190. https://doi.org/10.1023/A:1013072519889.

Tiwari, A., Fan, Z.-X., Jump, A.S., Zhou, Z.-K., 2017. Warming induced growth decline of Himalayan birch at its lower range edge in a semi-arid region of Trans-Himalaya, central Nepal. Plant Ecol. 218 (5), 621–633. https://doi.org/10.1007/s11258-017-0716-z.

Trouet, V., Oldenborgh, G.J.V., 2013. KNMI Climate Explorer: A web-based research tool for high-resolution paleoclimatology. Tree-Ring Res. 69 (1), 3–14. https://doi.org/10.3959/1536-1098-69.1.3.

van der Maaten-Theunissen, M., van der Maaten, E., Bouriaud, O., 2015. pointRes: An R package to analyze pointer years and components of resilience. Dendrochronologia 35, 34–38. https://doi.org/10.1016/j.dendro.2015.05.006.

Wang, W., Jia, M., Wang, G., Zhu, W., McDowell, N.G., 2017. Rapid warming forces contrasting growth trends of subalpine fir (*Abies fabri*) at higher- and lower-elevations in the eastern Tibetan Plateau. For. Ecol. Manag. 402, 135–144. https://doi.org/10.1016/j.foreco.2017.07.043.

Weigel, R., Muffler, L., Klisz, M., Kreyling, J., van der Maaten-Theunissen, M., Wilmking, M., van der Maaten, E., 2018. Winter matters: Sensitivity to winter climate and cold events increases towards the cold distribution margin of European beech (Fagus sylvaticaL.). J. Biogeogr. 45 (12), 2779–2790. https://doi.org/10.1111/jbi.13444.

Wigley, T.M., Briffa, K.R., Jones, P.D., 1984. On the average value of correlated time series, with applications in dendroclimatology and hydrometeorology. J. Clim. Appl. Meteorol. 23 (2), 201–213. https://doi.org/10.1175/1520-0450(1984)023%3C0201:OTAVOC%3E2.0.CO%3B2.

Wilmking, M., van der Maaten-Theunissen, M., van der Maaten, E., Scharnweber, T., Buras, A., Biermann, C., Trouillier, M., 2020. Global assessment of relationships between climate and tree growth. Glob. Change Biol. 26 (6), 3212–3220. https://doi.org/10.1111/gcb.15057.

Wood, S.N., 2017. Generalized Additive Models: an Introduction with R. Chapman and Hall/CRC, London, UK.

Yadav, R.R., Singh, J., Dubey, B., Chaturvedi, R., 2004. Varying strength of relationship between temperature and growth of high-level fir at marginal ecosystems in western Himalaya, India. Curr. Sci. 86 (8), 1152–1156.

Yang, B., He, M.H., Shishov, V., Tychkov, I., Vaganov, E., Rossi, S., Griessinger, J., 2017. New perspective on spring vegetation phenology and global climate change based on Tibetan Plateau tree-ring data. Proc. Nat. Acad. Sci. U.S.A. 114 (27), 6966–6971. https://doi.org/10.1073/pnas.1616608114.

Yang, R.-Q., Zhao, F., Fan, Z.-X., Panthi, S., Fu, P.-L., Bräuning, A., Li, Z.-S., 2022. Long-term growth trends of *Abies delavayi* and its physiological responses to a warming climate in the Cangshan Mountains, southwestern China. For. Ecol. Manag. 505, 119943 https://doi.org/10.1016/j.foreco.2021.119943.

Yu, D., Liu, J., Benard, J, L., Zhou, L., Zhou, W., Fang, X., Dai, L., 2013. Spatial variation and temporal instability in the climate–growth relationship of Korean pine in the Changbai Mountain region of Northeast China. For. Ecol. Manag. 300, 96–105. https://doi.org/10.1016/j.foreco.2012.06.032.

Zang, C., Biondi, F., 2015. Treeclim: an R package for the numerical calibration of proxy-climate relationships. Ecography 38 (4), 431–436. https://doi.org/10.1111/ecog.01335.

Zhang, Y., Wilmking, M., 2010. Divergent growth responses and increasing temperature limitation of Qinghai spruce growth along an elevation gradient at the northeast Tibet Plateau. For. Ecol. Manag. 260 (6), 1076–1082. https://doi.org/10.1016/j.foreco.2010.06.034.

Zhang, Y., Guo, M., Wang, X., Gu, F., Liu, S., 2017. Divergent tree growth response to recent climate warming of *Abies faxoniana* at alpine treelines in east edge of Tibetan Plateau. Ecol. Res. 33 (2), 303–311. https://doi.org/10.1007/s11284-017-1538-0.